RSC Advances

PAPER

View Article Online
View Journal | View Issue

Open Access Article. Published on 17 June 2019. Downloaded on 12/5/2025 12:57:05 AM.
This article is licensed under a Creative Commons Attribution-NonCommercial 3.0 Unported Licence.

Check for updates

Cite this: *RSC Adv.*, 2019, **9**, 18923

Synthesis and anticancer activity novel dimeric azatriperoxides†

Nataliya N. Makhmudiyarova,* Irina R. Ishmukhametova, Lilya U. Dzhemileva,* Tatyana V. Tyumkina, Vladimir A. D'yakonov, Askhat G. Ibragimov and Usein M. Dzhemilev

Received 19th April 2019
Accepted 4th June 2019

DOI: 10.1039/c9ra02950h

rsc.li/rsc-advances

An efficient method was developed for the synthesis of tetra(spirocycloalkane)-substituted α,ω-di(1,2,4,5,7,8-hexaoxa-10-azacycloundecan-10-yl)alkanes by a ring transformation reaction of 3,6-di(spirocycloalkane)-substituted 1,2,4,5,7,8,10-heptaoxacycloundecanes with α,ω-alkanediamines (1,4-butane-, 1,5-pentane-, 1,7-heptane-, 1,8-octane- and 1,10-decanediamines) catalyzed by $Sm(NO_3)_3/\gamma$-Al_2O_3. Using flow cytometry, it was shown for the first time that synthesized dimeric azatriperoxides are efficient apoptosis inducers with Jurkat, K562, U937, and Hek296.

Introduction

Cyclic peroxides are promising anti-cancer agents.[1–4] Antitumor activity was found for the well-known antimalarial drug artemisinin, which contains a peroxide moiety in the cycle.[5] The method of synthesis of *N*-aryl-substituted tetraoxazaspiroalkanes[6] developed by us allowed us to establish the antitumor activity of Ad-substituted *N*-aryl-tetraoxaspiroalkanes.[7] In the development of ongoing research in the field of the synthesis of nitrogen-containing di-[6] and triperoxides,[8] this report discusses the synthesis and anticancer activity of cyclic α,ω-di(azatriperoxy)alkanes.

The catalytic ring transformation reaction of pentaoxacanes and heptaoxadispiroalkanes with arylamines is an efficient method for the selective synthesis of novel *N*-substituted tetraoxazocanes and hexaoxazadispiroalkanes,[6–9] which are promising as biologically active compounds,[1–4] radical polymerization initiators,[10,11] and engine oil additives.[12] They are also interesting from a conformational point of view since their large rings can be stabilized in different conformations.[13] As a part of continuing research in our laboratory on design, synthesis and characterization of new drug molecules[6–9] of azaperoxides, we are extending our work to the design and synthesis of new cyclic peroxides to evaluate their anticancer activity and also to study their structures.

Prior to the beginning of our research, no data on the synthesis of tetra(spirocycloalkane)-substituted α,ω-bis-(1,2,4,5,7,8-hexaoxa-10-azacycloundecan-10-yl)alkanes were available from the literature.

Institute of Petrochemistry and Catalysis, Russian Academy of Sciences, 141 Prospekt Oktyabrya, 450075 Ufa, Russian Federation. E-mail: natali-mnn@mail.ru; dzhemilev@mail.ru

† Electronic supplementary information (ESI) available. See DOI: 10.1039/c9ra02950h

Results and discussion

In continuation of our research on the synthesis of new amino peroxides, and in order to develop an efficient method for the synthesis of spirocycloalkane-substituted α,ω-bis-(1,2,4,5,7,8-hexaoxa-10-azacycloundecan-10-yl)alkanes, we studied the ring transformation reaction of heptaoxadispiroalkanes with α,ω-alkanediamines under conditions of catalytic ring transformation reactions of pentaoxaspiroalkanes and hexaoxazadispiroalkanes, which we had carried out previously.[6–8] According to our experiments, the target spirocycloalkane-substituted macroheterocycles **10–23** can be selectively synthesized in high yields by the reaction of heptaoxadispiroalkanes **1–3** with α,ω-alkanediamines (1,2-ethane-, 1,4-butane-, 1,5-pentane-, 1,7-heptane-, 1,8-octane- and 1,10-decanediamines) **4–9** in the presence of catalysts based on d- and f-elements (Scheme 1). Spiroheptaoxacanes **1–3** were prepared by condensation of 1,1′-peroxy-bis(1-hydroperoxycycloalkanes)[14] with formaldehyde in the presence of $Sm(NO_3)_3 \cdot 6H_2O$ (0.5 mol%) as the catalyst for 6 h at ~20 °C in THF, according to the previously described method.[8]

As catalysts, we used $Sm(NO_3)_3 \cdot 6H_2O$ and γ-Al_2O_3-immobilized $Sm(NO_3)_3$ (the $Sm(NO_3)_3$ content on Al_2O_3 was 06 mmol g^{-1}). These catalysts were chosen because of their high activity

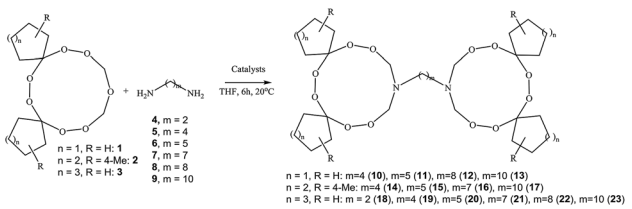

Scheme 1 Synthesis of α,ω-bis-(1,2,4,5,7,8-hexaoxa-10-azacycloundecan-10-yl)alkanes.

Open Access Article. Published on 17 June 2019. Downloaded on 12/5/2025 12:57:05 AM.
This article is licensed under a Creative Commons Attribution-NonCommercial 3.0 Unported Licence.

and selectivity observed in our previous studies.[6–8] Apart from these catalysts, we tested $La(NO_3)_3$, $TbCl_3 \cdot 6H_2O$, $Ho(NO_3)_3 \cdot 5H_2O$, $DyCl_3 \cdot 6H_2O$, and $NdCl_3$.

We found that 6,7,13,14,16,18,19-heptaoxadispiro[4.2.4^8.7^5]nonadecane **1** reacts with an equimolar amount of butane-1,4-diamine **5** (conditions: ~20 °C, THF, 6 h) in the presence of the $Sm(NO_3)_3 \cdot 6H_2O$ catalyst (5 mol%) to give 1,4-bis-(6,7,13,14,18,19-hexaoxa-16-azadispiro[4.2.4^8.7^5]nonadecan-16-yl)butane **10** in 84% yield. In the reactions catalyzed by the heterogeneous catalyst, 5 wt% $Sm(NO_3)_3/\gamma\text{-}Al_2O_3$, the yield of the target product **10** was 89%. Repeated use of the heterogeneous catalyst, $Sm(NO_3)_3/\gamma\text{-}Al_2O_3$ (three times) led to a considerable decrease in the yield of the target product **10**. The reaction was carried out in THF, because of good solubility of the stating 6,7,13,14,16,18,19-heptaoxadispiro[4.2.4^8.7^5]nonadecane **1**. When the $Sm(NO_3)_3 \cdot 6H_2O$ catalyst was replaced by other lanthanide salts [$La(NO_3)_3$, $TbCl_3 \cdot 6H_2O$, $Ho(NO_3)_3 \cdot 5H_2O$, $DyCl_3 \cdot 6H_2O$, $NdCl_3$], the yield of 1,4-bis-(6,7,13,14,18,19-hexaoxa-16-azadispiro[4.2.4^8.7^5]nonadecan-16-yl)butane **10** was 60–65% (Table 1).

Presumably, the mechanism of the catalytic ring transformation reaction of 6,7,13,14,16,18,19-heptaoxadispiro[4.2.4^8.7^5]nonadecane **1** with butane-1,4-diamine **5** includes coordination of the oxygen atom of compound **1** to the central ion of the catalyst[15] with electron density shift giving a carboxonium ion. The subsequent nucleophilic addition of the amine group of 1,4-butanediamine to the carbocation[16,17] gives rise to the C–N bond and affords the target 1,4-bis-(6,7,13,14,18,19-hexaoxa-16-azadispiro[4.2.4^8.7^5]nonadecan-16-yl)butane **10**.

Under the developed conditions [5 wt% $Sm(NO_3)_3/\gamma\text{-}Al_2O_3$, 20 °C, 6 h], the reaction of heptaoxadispiroalkane **1** with 1,5-pentanediamine **6**, 1,8-octanediamine **8** and 1,10-decanediamine **9** gives dimeric α,ω-bis-(6,7,13,14,18,19-hexaoxa-16-azadispiro[4.2.4^8.7^5]nonadecan-16-yl)alkanes **11–13** with a yield of 86, 80 and 83%, respectively. In order to extend the scope of applicability of the developed method and to find out whether this reaction can be carried out for other heptaoxadispiroalkanes, α,ω-diamines **4–9** were reacted with 3,12-dimethyl-7,8,15,16,18,20,21-heptaoxadispiro[5.2.5^9.7^6]henicosane **2** and 8,9,17,18,20,22,23-heptaoxadispiro[6.2.6^{10}.7^7]tricosane **3**. As a result, in the presence of the $Sm(NO_3)_3/\gamma\text{-}Al_2O_3$ catalyst [α,ω-diamine : heptaoxadispiroalkane : $Sm(NO_3)_3/\gamma\text{-}Al_2O_3$ molar ratio of 1 : 2 : 0.05], the reactions gave α,ω-bis-(3,12-dimethyl-7,8,15,16,20,21-hexaoxa-18-azadispiro[5.2.5^9.7^6]henicosan-18-yl)alkanes **14–17** and α,ω-bis-(8,9,17,18,22,23-hexaoxa-20-azadispiro[6.2.6^{10}.7^7]tricosan-20-yl)alkanes **18–23** in 75–82% yields.

The mass spectra of macroheterocycles **10–23** contain the corresponding molecular ion peaks. The ^{1}H NMR spectra exhibit signals in the ranges of 0.8–2.4 ppm, 2.6–3.5 ppm, and 4.6–5.5 ppm corresponding to the alkyl, N–CH_2 and N–CH_2O protons, respectively. For the series of compounds **10–23**, the proton signals are overlapping multiplets; the ^{13}C NMR spectra also exhibit an increased number of signals, which is attributable to the presence of a multicomponent conformational equilibrium. Previously, we confirmed this assumption for aryltriamino peroxides.[8] It is noteworthy that in the case of compounds **20–23**, containing bulky spiroheptacyclic moieties in the molecules, the NMR spectra at room temperature indicate the predominance of some conformers, since the methylene hydrogen atoms between the N and O heteroatoms in the 11-membered rings occur as two doublets at 4.7 and 4.8 ppm with the geminal constants $J = 12.0$ Hz (for example **20a**). In the ^{13}C NMR spectrum two signals of cyclic carbon atoms are observed as well, for example, for compound **20** there are signals at 87 and 90 ppm. On the basis of theoretical analysis of the conformer's energy (see ESI Fig. S1†), the structures of the most energetically favorable conformers were proposed, which can be observed in the NMR spectra by shifting the conformation equilibrium. The calculated structures are presented in Fig. 1.

To confirm this assumption, we calculated ^{1}H and ^{13}C NMR chemical shifts of the characteristic cyclic –N–CH_2–O– atoms (the results are presented in ESI Table S1†). The obtained

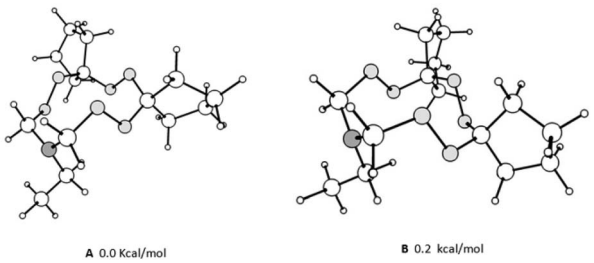

Fig. 1 Optimized structures of the lowest energy conformers of *N*-ethyl-6,7,13,14,18,19-hexaoxa-16-azadispiro[4.2.4^8.7^5]nonadecane.

Table 1 Effect of metal atom of the catalyst on the yield of 1,4-bis-(6,7,13,14,18,19-hexaoxa-16-azadispiro[4.2.4^8.7^5]nonadecan-16-yl)butane **10**

No	Catalyst	Yield[a] of **10**, %	No	Catalyst	Yield[a] of **10**, %
1	$Sm(NO_3)_3/\gamma\text{-}Al_2O_3$	89	8	$NdCl_3$	60
2	$Sm(NO_3)_3 \cdot 6H_2O$	84	9	$InCl_3$	46
3	$SnCl_4$	68	10	$ZnCl_2$	45
4	$La(NO_3)_3$	66	11	$AlCl_3$	40
5	$Ho(NO_3)_3 \cdot 5H_2O$	64	12	$FeCl_3 \cdot 6H_2O$	33
6	$TbCl_3 \cdot 6H_2O$	60	13	$CuCl_2 \cdot 5H_2O$	30
7	$DyCl_3 \cdot 6H_2O$	60	14	—	0

[a] Experimental conditions: **1** : **5** [M] molar ratio of 2 : 1 : 0.05; 20 °C; 6 h; in THF.

Open Access Article. Published on 17 June 2019. Downloaded on 12/5/2025 12:57:05 AM.
This article is licensed under a Creative Commons Attribution-NonCommercial 3.0 Unported Licence.

calculated data are in good agreement with the experimental ones. So, carbons between *N*,*O*-heteroatoms of the most energetically favorable conformers should resonate in an upfield range compared to the highest energy conformers. In addition, values of the observed and calculated chemical shifts of the corresponding diastereotopic protons are close. To estimate the cyclic inversion barrier for triperoxides, ^{1}H NMR spectra were recorded at 323 K (see ESI†). It was established that the spectra do not undergo significant changes, which indicates high barriers of conformational transitions, similar to the previously described *N*-arylhexaoxazadispiroalkanes.[3]

Cytotoxicity of peroxide based compounds is well known,[1–5] so we screened representative compounds for their cytotoxicity activity against Jurkat, K562, U937 and a conditionally normal Hek293 cell line and results are summarized in Table 2.

Hence, as one may observe from Table 2, regardless of what the substituents are, the initial 3,6-di(spirocycloalkane)-substituted 1,2,4,5,7,8,10-heptaoxacycloundecans **1–3** demonstrated nearly identical cytotoxicity against the cell lines Jurkat, K562 and U937, so that the IC_{50} values for the mentioned cells fell within a range of 5.93–8.12 μM, whereas the IC_{50} value for the Hek293 cells fell within a range of 14.29–18.26 μM, accordingly.

It is interesting that for the dimeric molecules of α,ω-di(1,2,4,5,7,8-hexaoxa-10-azacycloundecane-10-yl)alkanes **13**, **17**, and **23** synthesized hereby, cytotoxicity increased 2-4-fold in comparison with the original molecules. Thus, the dimer **23** constructed of two molecules, **3** and 1,10-decanediamine **9**, demonstrated the highest cytotoxicity.

In continuation of these studies, experiments were conducted to investigate influence of the test compounds on induction of apoptosis and the effects of them on the cell cycle, thus allowing us to understand, at least to some extent, whether cell death occurs by an apoptotic pathway or *via* necrosis. Induction of apoptosis has been studied by flow cytofluorimetry using dyes containing annexin V and 7-aminoactinomycin D (7AAD). Using annexin V together with 7AAD allowed for simultaneous determination of viable cells (negative by annexin V and by 7AAD), cells in the early stages of apoptosis (positive by annexin V and negative by 7AAD), as well as cells in the late apoptosis (positive by annexin V and by 7AAD) and/or necrosis (positive by 7AAD only).

To study the induction of apoptosis, compound **23** was selected due to its' most pronounced cytotoxicity against the cell lines utilized hereby (Fig. 2).

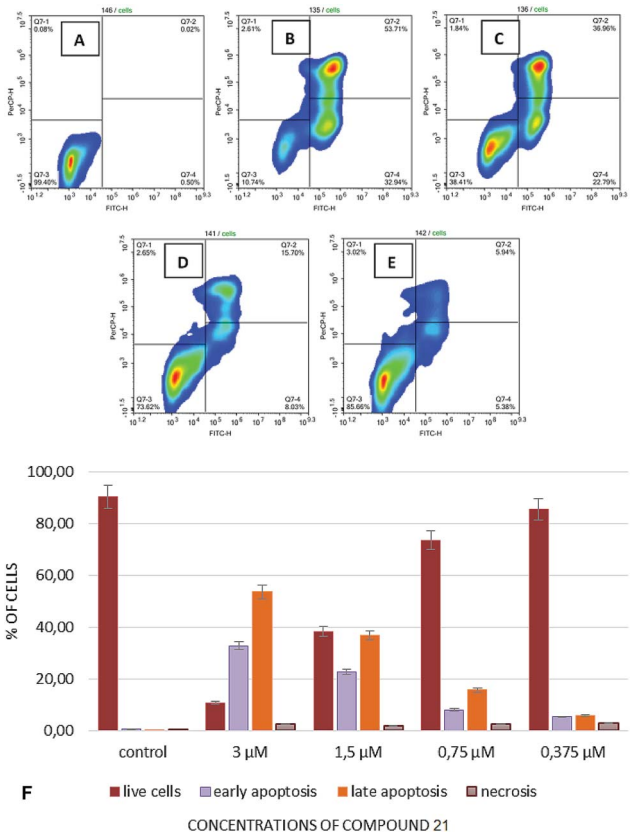

Fig. 2 Jurkat tumor cells treated with compound **23** in different concentrations and stained with annexin V/7AAD. Flow cytometry data (Q7-1, necrotic cells; Q7-2, late apoptotic cells; Q7-3, living cells; Q7-4, early apoptotic cells). (A) Control (without compound), (B) **23** (3.0 μM), (C) **23** (1.5 μM), (D) **23** (0.75 μM), (E) **23** (0.375 μM). (F) Flow cytometry histogram represents the percentage of cells in each apoptosis phase. The histogram shows the apoptosis rate (%); $^{**}P < 0.05$ when compared with the control group ($n = 5$).

Considering the results on cytotoxicity obtained with the compounds under study, we undertook a more detailed investigation on the apoptosis-inducing activity of compound **23** against T-cell leukemia cells. The highest percentage of cells in the stages of early and late apoptosis was observed upon addition of compound **23** into the cell culture Jurkat at a concentration of 3 μL and constituted 32.94% and 53.71%, respectively (Fig. 2B and G). The percentage of necrotic cells was virtually independent of concentration of the test compounds and constituted

Table 2 Cytotoxic activities *in vitro* of compounds **1–3**, **13**, **17**, and **23** measured on tumor cell cultures (Jurkat, K562, U937, Hek293) (μM)

C-d	Jurkat (IC_{50}, μM)	K562 (IC_{50}, μM)	U937 (IC_{50}, μM)	HEK293 (IC_{50}, μM)
1	6.33 ± 0.12	6.04 ± 0.18	5.93 ± 0.21	18.26 ± 0.31
13	3.24 ± 0.24	3.44 ± 0.17	3.02 ± 0.13	15.27 ± 0.29
2	7.62 ± 0.14	8.12 ± 0.34	7.41 ± 0.11	14.29 ± 0.54
17	3.12 ± 0.25	3.27 ± 0.15	2.98 ± 0.17	12.25 ± 0.48
3	7.18 ± 0.17	7.49 ± 0.21	6.88 ± 0.27	16.37 ± 0.28
23	1.56 ± 0.16	1.74 ± 0.11	1.41 ± 0.13	5.42 ± 0.37

Open Access Article. Published on 17 June 2019. Downloaded on 12/5/2025 12:57:05 AM.
This article is licensed under a Creative Commons Attribution-NonCommercial 3.0 Unported Licence.

approximately 2–3% in experiments that involved adding compound **23** in concentrations ranging from 3 μM to 0.375 μM.

Fig. 3 demonstrates the results obtained from studies on the cell cycle kinetics' indicators for the Jurkat cell line, determined by flow DNA-cytometry 24 hours after the treatment of those cells with compound **23** in various concentrations.

Cell cycle indicators for the Jurkat culture in the samples treated with compound **23** at a concentration of 3.0 μM were characterized by a significant predominance of cells in the G0 phase (sub-G0–G1 interval), by a pronounced reduction of G1 and G2 populations, and by accumulation of cells in the S phase. This effect was dose-dependent and the tendency for cell accumulation in the S-phase was preserved despite a reduction in concentration of test compound **23**. Thus, since compound **23** is an efficient apoptosis-inducing agent and, apparently, causes a checkpoint-dependent inhibition of the cell cycle in all its phases, it may be concluded that compound **23** possesses high anticancer potential.

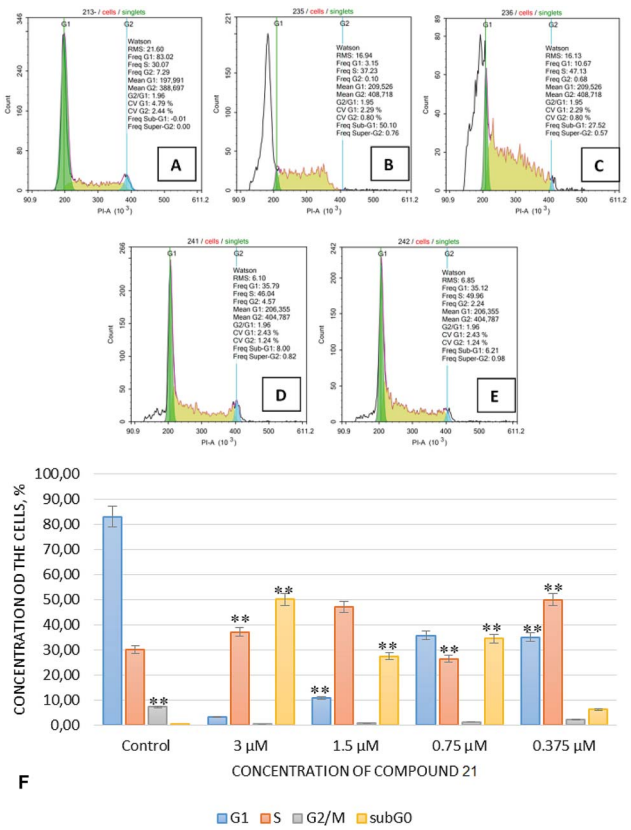

Fig. 3 Cell cycle phases of Jurkat cells treated with compound **23**. (A) Control (without compound), (B) **23** (3.0 μM), (C) **23** (1.5 μM), (D) **23** (0.75 μM), (E) **23** (0.375 μM). (F) Flow cytometry histogram represents the percentage of cells in each cell cycle phase (The incubation time of cpd **23** with the cells was 24 h). Data are presented with the means ± SD and mean values of three independent experiments. $^{**}P < 0.01$, compared with the control group ($n = 5$). The G0/G1%, S% and G2 + M% phases of the cells were analyzed using flow cytometry. Flow cytometric histograms are representative of 3 separate experiments.

Conclusions

The reaction presented above is the first ever reported ring transformation reaction of heptaoxadispiroalkanes with α,ω-diamines catalyzed by Sm compounds that simultaneously involves both amino groups and provides a potentially useful one-pot synthesis of spirocycloalkane-substituted α,ω-bis-(1,2,4,5,7,8-hexaoxa-10-azacycloundecan-10-yl)alkanes – which, in consequence of their aminoperoxy groups, are expected to exhibit interesting biological properties. In addition, it was shown that the synthesized dimeric molecules exhibited high cytotoxic activity against Jurkat, K562, and U937 tumor cultures and conditionally normal Hek293 cell line, as well as induced apoptosis and caused cell cycle arrest, affecting all its phases.

Experimental section

General remarks

All reactions were performed at room temperature in air in round-bottom flasks equipped with a magnetic stir bar. The NMR spectra, including two-dimensional homo- (COSY, NOESY) and heteronuclear (HSQC, HMBC) spectra, were recorded on a Bruker Avance 500 spectrometer at 500.17 MHz for ^{1}H and 125.78 MHz for ^{13}C according to standard Bruker procedures. $CDCl_3$ was used as the solvent, and tetramethylsilane, was the internal standard. Mixing time for the NOESY experiments was 0.3 s. Mass spectra were recorded on a Bruker Autoflex III MALDI TOF/TOF instrument with α-cyano-4-hydroxycinnamic acid as a matrix. Samples were prepared by the dried droplet method. C, H, and N were quantified by a Carlo Erba 1108 analyzer. The oxygen content also was determined on a Carlo Erba 1108 analyzer. Reaction progress was monitored by TLC on Sorbfil (PTSKh-AF-A) plates, with a 5 : 1 hexane : EtOAc mixture as the eluent and visualization with I_2 vapor. For column chromatography, silica gel MACHEREY-NAGEL (0.063–0.2 mm) was used.

All calculations were carried out using the program Gaussian 09. Geometric parameter optimization, vibrational frequency analysis, and calculation of entropy and thermodynamic corrections to the total energy of the compounds were carried out on the B3LYP functional[18] using the 6-31G(d,p) basis set. No limitation was imposed on the changes in the geometric parameters of the subsystems studied. Thermodynamic parameters were determined at 298 K. The minima were confirmed through calculation of the force constant (Hessian) matrix and analysis of the resulting frequencies. All minima were verified to have no negative frequencies. Visualization of quantum chemical data was carried out with the program ChemCraft.[19]

Synthesis of heptaoxadispiroalkanes **1–3** was as reported in the literature.[20] THF was freshly distilled over $LiAlH_4$. $Sm(NO_3)_3$/γ-Al_2O_3 catalyst was synthesized by impregnating a porous Al_2O_3 carrier with an aqueous solution of $Sm(NO_3)_3 \times 6H_2O$ followed by a heat treatment at 400 °C for 4 hours. The content of the active component Sm^{3+} was 0.60–0.69 mmol g^{-1} of catalyst.

Open Access Article. Published on 17 June 2019. Downloaded on 12/5/2025 12:57:05 AM.
This article is licensed under a Creative Commons Attribution-NonCommercial 3.0 Unported Licence.

Ring transformation of heptaoxaspirocycloalkanes with alkane-α,ω-diamines catalyzed by $Sm(NO_3)_3/\gamma$-Al_2O_3

General procedure: A Schlenk vessel mounted on a magnetic stirrer was charged under argon with THF (5 mL), $Sm(NO_3)_3/\gamma$-Al_2O_3 (5 wt%), alkane-α,ω-diamines (1 mmol), and heptaoxaspirocycloalkane (2 mmol). The reaction mixture was stirred at ~20 °C for 6 h and then THF was evaporated. Then Et_2O (10 mL) was added and the mixture was washed with water (4 × 5 mL). The organic layer was separated and purified by column chromatography on SiO_2 using 10 : 1 PE : Et_2O as the eluent to isolate the pure heterocyclic product (compounds **10–23**). Progress of reactions was monitored by TLC, with a 5 : 1 hexane : EtOAc mixture for the eluent (compounds **10–23**) and visualization was performed with I_2 vapor.

1,4-Bis-(6,7,13,14,18,19-hexaoxa-16-azadispiro[4.2.4^8.7^5]nonadecan-16-yl)butane 10

Yellow oil, 0.378 g (63% yield), R_f 0.88 (PE/Et_2O = 10/1). ^{1}H NMR (500.17 MHz, $CDCl_3$): δ = 1.69–1.75 (m, 24H), 1.84 and 2.09 (br.s, 4H), 2.15–2.25 (m, 8H), 2.95–3.01 and 3.51–3.53 (m, 4H), 4.82–5.37 (m, 8H). ^{13}C NMR (125.78 MHz, $CDCl_3$): δ = 22.8, 24.6, 24.3, 33.5, 32.9, 33.2, 33.7, 49.0, 84.6, 95.4, 119.3, 118.7. MALDI TOF/TOF, *m*/*z*: 603 [M − H]$^+$. Anal. calcd. for $C_{28}H_{48}N_2O_{12}$: C, 55.62; H, 8.00; N, 4.63%. Found: C, 55.57; H, 7.95; N, 4.57%.

1,5-Bis-(6,7,13,14,18,19-hexaoxa-16-azadispiro[4.2.4^8.7^5]nonadecan-16-yl)pentane 11

Yellow oil, 0.489 g (79% yield), R_f 0.88 (PE/Et_2O = 10/1). ^{1}H NMR (500.17 MHz, $CDCl_3$): δ = 1.25–1.33 (m, 4H) and 1.67–1.77 (m, 14H), 1.47–1.53 (m, 4H), 1.62–1.65 and 2.14–2.17 (m, 16H), 2.96–3.02 and 3.19–3.24 (m, 4H), 4.80–4.89 and 4.93–5.22 (m, 8H). ^{13}C NMR (125.78 MHz, $CDCl_3$): δ = 23.9, 24.4, 28.2, 32.9, 33.1, 51.5, 88.2, 90.5, 113.7. MALDI TOF/TOF, *m*/*z*: 617 [M − H]$^+$. Anal. calcd. for $C_{29}H_{50}N_2O_{12}$: C, 56.30; H, 8.15; N, 4.53%. Found: C, 56.25; H, 8.13; N, 4.49%.

1,8-Bis-(6,7,13,14,18,19-hexaoxa-16-azadispiro[4.2.4^8.7^5]nonadecan-16-yl)octane 12

Colorless oil, 0.455 g (69% yield), R_f 0.86 (PE/Et_2O = 10/1). ^{1}H NMR (500.17 MHz, $CDCl_3$): δ = 1.65–1.77 (m, 16H), 1.65–1.70 and 2.16–2.19 and 2.21–2.24 (m, 16H), 1.28–1.36 (m, 8H), 1.47–1.50 (m, 4H), 2.95–3.03 and 3.19–3.25 (m, 4H), 4.82–4.91 and 4.93–5.19 (m, 8H). ^{13}C NMR (125.78 MHz, $CDCl_3$): δ = 24.6, 24.4, 32.5, 32.9, 26.9, 28.3, 29.7, 51.6, 88.3, 119.3, 119.7. MALDI TOF/TOF, *m*/*z*: 659 [M − H]$^+$. Anal. calcd. for $C_{32}H_{56}N_2O_{12}$: C, 58.16; H, 8.54; N, 4.24%. Found: C, 58.14; H, 8.51; N, 4.21%.

1,10-Bis-(6,7,13,14,18,19-hexaoxa-16-azadispiro[4.2.4^8.7^5]nonadecan-16-yl)decane 13

Colorless oil, 0.495 g (72% yield), R_f 0.84 (PE/Et_2O = 10/1). ^{1}H NMR (500.17 MHz, $CDCl_3$): δ = 1.63–1.77 (m, 16H), 1.63–1.69 and 1.95–2.08 and 2.14–2.23 (m, 16H), 1.20–1.23 (m, 12H), 1.45–1.48 (m, 4H), 2.95–3.01 and 3.17–3.22 (m, 4H), 4.80–4.89 and 4.91–5.20 (m, 8H). ^{13}C NMR (125.78 MHz, $CDCl_3$): δ = 24.5, 24.6, 24.5, 24.4, 33.1, 33.4, 33.3, 32.9, 26.9, 28.3, 29.4, 29.5, 51.5, 88.2, 90.5, 119.6, 119.2, 122.4. MALDI TOF/TOF, *m*/*z*: 687 [M − H]$^+$. Anal. calcd. for $C_{34}H_{60}N_2O_{12}$: C, 59.28; H, 8.78; N, 4.07%. Found: C, 59.25; H, 8.76; N, 4.05%.

1,4-Bis-(3,12-dimethyl-7,8,15,16,20,21-hexaoxa-18-azadispiro[5.2.5^9.7^6]henicosan-18-yl)butane 14

Colorless oil, 0.529 g (74% yield), R_f 0.87 (PE/Et_2O = 10/1). ^{1}H NMR (500.17 MHz, $CDCl_3$): δ = 0.76–0.77 and 0.87–0.88 (m, 12H), 1.39–1.49 (m, 4H), 1.91–2.00 and 0.97–1.49 (m, 4H), 1.84–1.87 and 1.29–1.34 (m, 16H), 2.18–2.24 (m, 16H), 2.83–2.88 and 3.05–3.08 (m, 4H), 4.60–4.96 (m, 8H). ^{13}C NMR (125.78 MHz, $CDCl_3$): δ = 20.9, 21.4, 25.6, 25.2, 31.0, 31.5, 30.7, 30.9, 34.6, 40.6, 51.1, 88.0, 108.2, 110.4. MALDI TOF/TOF, *m*/*z*: 715 [M − H]$^+$. Anal. calcd. for $C_{36}H_{64}N_2O_{12}$: C, 60.31; H, 9.00; N, 3.91%. Found: C, 60.29; H, 8.98; N, 3.89%.

1,5-Bis-(3,12-dimethyl-7,8,15,16,20,21-hexaoxa-18-azadispiro[5.2.5^9.7^6]henicosan-18-yl)pentane 15

Colorless oil, 0.452 g (62% yield), R_f 0.85 (PE/Et_2O = 10/1). ^{1}H NMR (500.17 MHz, $CDCl_3$): δ = 0.92–0.94 (m, 12H), 1.27–1.30 (m, 2H), 1.49–1.52 (m, 4H), 1.42–1.44 (m, 16H), 1.10–1.30 and 1.57–1.65 and 2.08–2.17 (m, 20H), 2.95–3.03 and 3.18–3.23 (m, 4H), 4.76–4.93 and 5.08–5.13 (m, 8H). ^{13}C NMR (125.78 MHz, $CDCl_3$): δ = 21.5, 24.3, 30.8, 31.0, 31.2, 31.5, 31.6, 51.4, 88.3, 90.4, 108.6, 110.7. MALDI TOF/TOF, *m*/*z*: 729 [M − H]$^+$. Anal. calcd. for $C_{37}H_{66}N_2O_{12}$: C, 60.80; H, 9.10; N, 3.83%. Found: C, 60.75; H, 9.05; N, 3.80%.

1,7-Bis-(3,12-dimethyl-7,8,15,16,20,21-hexaoxa-18-azadispiro[5.2.5^9.7^6]henicosan-18-yl)heptane 16

Colorless oil, 0.435 g (58% yield), R_f 0.86 (PE/Et_2O = 10/1). ^{1}H NMR (500.17 MHz, $CDCl_3$): δ = 0.93–0.94 (m, 12H), 1.27–1.30 (m, 6H), 1.43–1.49 (m, 16H), 1.27–1.49 and 2.09–2.11 (m, 8H), 1.57–1.66 and 2.15–2.18 (m, 16H), 2.95–3.04 and 3.17–3.25 (m, 4H), 4.77–4.89 and 4.91–5.13 (m, 8H). ^{13}C NMR (125.78 MHz, $CDCl_3$): δ = 26.9, 28.3, 29.3, 30.6, 31.1, 31.6, 51.4, 88.3, 90.5, 108.5, 110.7. MALDI TOF/TOF, *m*/*z*: 757 [M − H]+. Anal. calcd. for $C_{39}H_{70}N_2O_{12}$: C, 61.72; H, 9.30; N, 3.69%. Found: C, 61.67; H, 9.25; N, 3.62%.

1,10-Bis-(3,12-dimethyl-7,8,15,16,20,21-hexaoxa-18-azadispiro[5.2.5^9.7^6]henicosan-18-yl)decane 17

Colorless oil, 0.552 g (69% yield), R_f 0.87 (PE/Et_2O = 10/1). ^{1}H NMR (500.17 MHz, $CDCl_3$): δ = 0.74–0.91 (m, 12H), 1.08–1.59 (m, 48H), 2.03–1.12 (m, 4H), 2.89–2.98 and 3.11–3.16 (m, 4H), 4.70–5.06 (m, 8H). ^{13}C NMR (125.78 MHz, $CDCl_3$): δ = 21.5, 26.9, 28.3, 29.4, 29.5, 29.2, 30.8, 31.0, 31.6, 31.5, 31.4, 51.4, 82.2, 90.3, 90.4, 108.3, 110.5, 110.9. MALDI TOF/TOF, *m*/*z*: 800 [M − H]$^+$. Anal. calcd. for $C_{42}H_{76}N_2O_{12}$: C, 62.97; H, 9.56; N, 3.50%. Found: C, 62.95; H, 9.53; N, 3.48%.

1,2-Bis(8,9,17,18,22,23-hexaoxa-20-azadispiro[6.2.6^{10}.7^7]tricosan-20-yl)ethane 18

Colorless oil, 0.488 g (71% yield), R_f 0.85 (PE/Et_2O = 10/1). ^{1}H NMR (500.17 MHz, $CDCl_3$): δ = 1.43–1.47 (m, 16H), 1.53–1.66

Open Access Article. Published on 17 June 2019. Downloaded on 12/5/2025 12:57:05 AM.
This article is licensed under a Creative Commons Attribution-NonCommercial 3.0 Unported Licence.

(m, 16H), 1.89–1.96 and 2.14–2.19 (m, 16H), 3.12–3.15 and 3.29–3.35 (m, 4H), 4.75–4.91 (m, 8H). ^{13}C NMR (125.78 MHz, $CDCl_3$): δ = 22.7, 29.9, 30.1, 32.3, 32.5, 50.0, 85.8, 88.1, 114.0, 115.2. MALDI TOF/TOF, *m*/*z*: 687 [M − H]$^+$. Anal. calcd. for $C_{34}H_{60}N_2O_{12}$: C, 59.28; H, 8.78; N, 4.07%. Found: C, 59.26; H, 8.75; N, 4.04%.

1,4-Bis-(8,9,17,18,22,23-hexaoxa-20-azadispiro[6.2.6^{10}.7^7]tricosan-20-yl)butane 19

White solid, 0.497 g (70% yield), mp 99–100 °C, R_f 0.85 (PE/Et_2O = 10/1). ^{1}H NMR (500.17 MHz, $CDCl_3$): δ = 1.43–1.48 (m, 4H), 1.43–1.70 (m, 16H), 1.53–1.69 (m, 16H), 1.53–1.69 and 2.09–2.18 (m, 16H), 2.95–3.03 and 3.20–3.24 (m, 2H), 2.99–3.03 and 3.48–3.53 (m, 2H), 4.76–4.92 and 5.10–5.18 and 4.80–4.83 (m, 8H). ^{13}C NMR (125.78 MHz, $CDCl_3$): δ = 25.8, 25.4, 22.8, 22.7, 22.9, 30.1, 30.0, 30.2, 32.8, 33.4, 51.4, 49.1, 87.9, 84.4, 112.7, 113.0, 113.9. MALDI TOF/TOF, *m*/*z*: 715 [M − H]$^+$. Anal. calcd. for $C_{36}H_{64}N_2O_{12}$: C, 60.31; H, 9.00; N, 3.91%. Found: C, 60.28; H, 8.95; N, 3.87%.

1,5-Bis-(8,9,17,18,22,23-hexaoxa-20-azadispiro[6.2.6^{10}.7^7]tricosan-20-yl)pentane 20

White oil, 0.584 g (80% yield), R_f 0.86 (PE/Et_2O = 10/1). ^{1}H NMR (500.17 MHz, $CDCl_3$): δ = 1.25–1.28 (m, 2H), 1.43–1.50 (m, 4H), 1.43–1.71 (m, 16H), 1.51–1.62 (m, 16H), 1.61–1.64 and 2.13–2.18 (m, 16H), 2.96–3.01 and 3.17–3.22 (m, 4H), 4.76 and 4.84 (d, J = 12.0 Hz, 4H), 4.89 and 5.07 (d, J = 12.0 Hz, 4H). ^{13}C NMR (125.78 MHz, $CDCl_3$): δ = 22.7, 22.8, 24.3, 28.1, 28.2, 30.0, 30.1, 30.4, 32.4, 87.9, 90.4, 113.8. MALDI TOF/TOF, *m*/*z*: 729 [M − H]$^+$. Anal. calcd. for $C_{37}H_{66}N_2O_{12}$: C, 60.80; H, 9.10; N, 3.83%. Found: C, 60.75; H, 9.04; N, 3.79%.

1,7-Bis-(8,9,17,18,22,23-hexaoxa-20-azadispiro[6.2.6^{10}.7^7]tricosan-20-yl)heptane 21

Yellow oil, 0.570 g (75% yield), R_f 0.88 (PE/Et_2O = 10/1). ^{1}H NMR (500.17 MHz, $CDCl_3$): δ = 1.29 (m, 4H), 1.43–1.49 (m, 4H), 1.43–1.72 (m, 16H), 1.52–1.62 (m, 16H), 1.57–1.62 and 2.13–2.18 (m, 16H), 1.67–1.72 (m, 2H), 2.95–3.01 and 3.16–3.21 (m, 4H), 4.77 and 4.85 (d, J = 8.0 Hz, 4H), 4.90 and 5.07 (d, J = 12.0 Hz, 4H). ^{13}C NMR (125.78 MHz, $CDCl_3$): δ = 22.7, 22.8, 24.3, 26.9, 28.3, 30.1, 30.0, 30.4, 32.4, 32.8, 51.6, 88.0, 90.4, 113.8, 112.7. MALDI TOF/TOF, *m*/*z*: 757 [M − H]$^+$. Anal. calcd. for $C_{39}H_{70}N_2O_{12}$: C, 61.72; H, 9.30; N, 3.69%. Found: C, 61.68; H, 9.25; N, 3.67%.

1,8-Bis-(8,9,17,18,22,23-hexaoxa-20-azadispiro[6.2.6^{10}.7^7]tricosan-20-yl)octane 22

Colorless oil, 0.462 g (60% yield), R_f 0.90 (PE/Et_2O = 10/1). ^{1}H NMR (500.17 MHz, $CDCl_3$): δ = 1.27 (m, 8H), 1.40–1.47 (m, 4H), 1.40–1.66 (m, 16H), 1.50–1.66 (m, 16H), 1.52–1.63 and 2.12–2.16 (m, 16H), 2.93–2.99 and 3.14–3.20 (m, 4H), 4.75 and 4.83 (d, J = 8.0 Hz, 4H), 4.88 and 5.05 (d, J = 12.0 Hz, 4H). ^{13}C NMR (125.78 MHz, $CDCl_3$): δ = 22.7, 26.9, 27.9, 28.3, 29.8, 29.9, 30.1, 32.4, 32.8, 51.6, 87.9, 90.4, 113.8, 112.7. MALDI TOF/TOF, *m*/*z*: 772 [M − H]$^+$. Anal. calcd. for $C_{40}H_{72}N_2O_{12}$: C, 61.72; H, 9.30; N, 3.69%. Found: C, 61.66; H, 9.25; N, 3.63%.

1,10-Bis-(8,9,17,18,22,23-hexaoxa-20-azadispiro[6.2.6^{10}.7^7]tricosan-20-yl)decane 23

Colorless oil, 0.688 mg (86% yield), R_f 0.87 (PE/Et_2O = 10/1). ^{1}H NMR (500.17 MHz, $CDCl_3$): δ = 1.27 (m, 12H), 1.44–1.46 (m, 4H), 1.42–1.62 (m, 16H), 1.52–1.58 (m, 16H), 1.58–1.63 and 2.14–2.18 (m, 16H), 2.95–3.01 and 3.16–3.22 (m, 4H), 4.91 and 5.07 (d, J = 14.0 Hz, 8H), 4.85 and 4.78 (d, J = 12.0 Hz, 8H). ^{13}C NMR (125.78 MHz, $CDCl_3$): δ = 22.7, 22.8, 26.9, 28.4, 29.4, 29.5, 30.0, 30.1, 32.4, 32.8, 51.6, 49.5, 87.9, 90.4, 112.7, 113.8. MALDI TOF/TOF, *m*/*z*: 800 [M − H]$^+$. Anal. calcd. for $C_{42}H_{76}N_2O_{12}$: C, 62.97; H, 9.56; N, 3.50%. Found: C, 62.93; H, 9.51; N, 3.46%.

Bioassay data

Cell culturing. Human cancer cell line HeLa was obtained from the HPA Culture Collections (UK). Cells (U937, K562, Jurkat and HEK293) were purchased from the Russian Cell Culture Collection (Institute of Cytology of the Russian Academy of Sciences) and cultured according to standard protocols and sterile techniques. The cell lines were shown to be free of viral contamination and mycoplasma. HEK293 cell line was cultured as monolayers and maintained in Dulbecco's modified Eagle's medium (DMEM, Gibco BRL) supplemented with 10% fetal bovine serum and 1% penicillin–streptomycin solution at 37 °C in a humidified incubator under a 5% CO_2 atmosphere. Cells were maintained in RPMI 1640 (Jurkat, K562, U937) (Gibco) supplemented with 4 μM glutamine, 10% FBS (Sigma) and 100 units per mL penicillin–streptomycin (Sigma). All types of cells were grown in an atmosphere of 5% CO_2 at 37 °C. The cells were subcultured for 2–3 days intervals. Adherent cells (HEK293) were suspended using trypsin/EDTA and counted after they reached 80% confluency. Cells were then seeded in 24 well plates at 5×10^4 cells per well and incubated overnight. Jurkat, K562, U937 cells were subcultured at 2-day intervals with a seeding density of 1×10^5 cells per 24 well plates in RPMI with 10% FBS.

Cytotoxicity assay. Viability (live/dead) assessment was performed by staining cells with 7-AAD (7-aminoactinomycin D) (Biolegend). After treatment cells were harvested, washed 1–2 times with phosphate-buffered saline (PBS) and centrifuged at 400*g* for 5 min. Cell pellets were resuspended in 200 μL of flow cytometry staining buffer (PBS without Ca^{2+} and Mg^{2+}, 2.5% FBS) and stained with 5 μL of 7-AAD staining solution for 15 min at room temperature in the dark. Samples were acquired on a NovoCyte TM 2000 Flow Cytometry System (ACEA) equipped with 488 nm argon laser. Detection of 7-AAD emission was collected through a 675/30 nm filter in the FL4 channel.

Viability and apoptosis. Apoptosis was studied using flow cytometric analysis of annexin V and 7-aminoactinomycin D staining. After treatment, cells from 24 h were harvested, washed 1–2 times with phosphate-buffered saline (PBS) and centrifuged at 400 g for 5 min. Cell pellets were resuspended in a 200 μL of flow cytometry staining buffer (PBS without Ca^{2+} and Mg^{2+}, 2.5% FBS). Then, 200 μL of Guava Nexin reagent (Millipore, Bedford, MA, USA) was added to 5 × 105 cells in 200 μL, and the cells were incubated with the reagent for 20 min at room temperature in the dark. At the end of incubation, the cells were analyzed on a NovoCyte TM 2000 Flow Cytometry System (ACEA).

Open Access Article. Published on 17 June 2019. Downloaded on 12/5/2025 12:57:05 AM.
This article is licensed under a Creative Commons Attribution-NonCommercial 3.0 Unported Licence.

Cell cycle analysis. Cell cycle was analyzed using the method of propidium iodide staining.[21] After treatment, cells after 24 h were harvested, washed 1–2 times with phosphate-buffered saline (PBS) and centrifuged at 400 g for 5 min. Cell pellets were resuspended in 200 μL of flow cytometry staining buffer (PBS without Ca^{2+} and Mg^{2+}, 2.5% FBS). Then, cells were plated in 24-well round bottom plates at a density of 10×10^5 cells per well, centrifuged at 450 g for 5 min, and fixed with ice-cold 70% ethanol for 24 h at 0 °C. Cells were then washed with PBS and incubated for 30 min at room temperature with 250 μL of Guava Cell Cycle Reagent (Millipore) in the dark. Samples were analyzed with a NovoCyte TM 2000 Flow Cytometry System (ACEA).

Conflicts of interest

There are no conflicts to declare.

Acknowledgements

This work was financially supported by the Russian Science Foundation (RSF projects 18-73-00014). The structural studies of the synthesized compounds were performed with the use of Collective Usage Centre "Agidel" at the Institute of Petrochemistry and Catalysis of RAS. The anticancer activity studies of the synthesized compounds were performed in Laboratory of molecular design and biological screening of candidate substances for the pharmaceutical industry at the Institute of Petrochemistry and Catalysis of RAS.

Notes and references

1 P. Coghi, I. A. Yaremenko, P. Prommana, P. S. Radulov, M. A. Syroeshkin, Y. J. Wu, J. Y. Gao, F. M. Gordillo-Martinez, S. Mok, V. K. W. Wong, C. Uthaipibull and A. O. Terent'ev, *ChemMedChem*, 2018, **13**, 902–908.
2 V. A. Vil', I. A. Yaremenko, A. I. Ilovaisky and A. O. Terent'ev, *Molecules*, 2017, **22**, 1881–1919.
3 V. A. Vil', I. A. Yaremenko, A. I. Ilovaisky and A. O. Terent'ev, Synthetic Strategies for Peroxide Ring Construction in Artemisinin, *Molecules*, 2017, **22**, 117–136.
4 I. A. Yaremenko, M. A. Syroeshkin, D. O. Levitsky, F. Fleury and A. O. Terent'ev, *Med. Chem. Res.*, 2017, **26**, 170–179.
5 M. P. Crespo-Ortiz and M. Q. Wei, *J. Biomed. Biotechnol.*, 2012, 1–18.
6 N. N. Makhmudiyarova, G. M. Khatmullina, R. Sh. Rakhimov, E. S. Meshcheryakova, A. G. Ibragimov and U. M. Dzhemilev, *Tetrahedron*, 2016, **72**, 3277–3281.
7 T. V. Tyumkina, N. N. Makhmudiyarova, G. M. Kiyamutdinova, E. S. Meshcheryakova, K. Sh. Bikmukhametov, M. F. Abdullin, L. M. Khalilov, A. G. Ibragimov and U. M. Dzhemilev, *Tetrahedron*, 2018, **74**, 1749–1758.
8 N. N. Makhmudiyarova, I. R. Ishmukhametova, T. V. Tyumkina, A. G. Ibragimov and U. M. Dzhemilev, *Tetrahedron Lett.*, 2018, **59**, 3161–3164.
9 A. R. Tulyabaev, K. Sh. Bikmukhametov, E. S. Mescheryakova, N. N. Makhmudiyarova, R. Sh. Rakhimov and L. M. Khalilov, *CrystEngComm*, 2018, **20**, 3207–3217.
10 G. L. Ellis, R. Amewu, S. Sabbani, P. A. Stocks, A. Shone, D. Stanford, P. Gibbons, J. Davies, L. Vivas, S. Charnand, E. Bongard, C. Hall, K. Rimmer, S. Lozanom, M. Jesus, D. Gargallo, S. A. Ward and P. M. O'Neill, *J. Med. Chem.*, 2008, **51**, 2170–2177.
11 I. Opsenica, D. Opsenica, C. A. Lanteri, L. Anova, W. K. Milhous, K. S. Smith and B. A. Solaja, *J. Med. Chem.*, 2008, **51**, 6216–6219.
12 A. B. Rode, K. Chung, Y. W. Kim and I. S. Hong, *Energy Fuels*, 2010, **24**, 1636–1639.
13 C. Sh. Neupane and S. K. Awasthi, *Tetrahedron*, 2012, **53**, 6067–6070.
14 A. O. Terent'ev, M. M. Platonov, E. J. Sonneveld, R. Peschar, V. V. Chernyshev, Z. A. Starikova and G. I. Nikishin, *J. Org. Chem.*, 2007, **72**, 7237–7243.
15 (*a*) S. Oda, J. Franke and M. Krishce, *J. Chem. Sci.*, 2016, **7**, 136–141; (*b*) S. Vojacek, K. Beese, Z. Alhalabi, S. Swyter, A. Bodtke, C. Carola Schulzke, M. Jung, W. Sippl and A. Link, *Arch. Pharm.*, 2017, **350**, e1700097.
16 U. Wellmar, *J. Heterocycl. Chem.*, 1998, **35**, 1531–1532.
17 K. Krohn and S. Cludius-Brandt, *Synthesis*, 2010, **8**, 1344–1348.
18 M. J. Frisch, G. W. Trucks, H. B. Schlegel, G. E. Scuseria, M. A. Robb, J. R. Cheeseman, G. Scalmani, V. Barone, B. Mennucci, G. A. Petersson, H. Nakatsuji, M. Caricato, X. Li, H. P. Hratchian, A. F. Izmaylov, J. Bloino, G. Zheng, J. L. Sonnenberg, M. Hada, M. Ehara, K. Toyota, R. Fukuda, J. Hasegawa, M. Ishida, T. Nakajima, Y. Honda, O. Kitao, H. Nakai, T. Vreven, J. A. Montgomery, J. E. Peralta Jr, F. Ogliaro, M. Bearpark, J. J. Heyd, E. Brothers, K. N. Kudin, V. N. Staroverov, T. Keith, R. Kobayashi, J. Normand, K. Raghavachari, A. Rendell, J. C. Burant, S. S. Iyengar, J. Tomasi, M. Cossi, N. Rega, J. M. Millam, M. Klene;, J. E. Knox, J. B. Cross, V. Bakken, C. Adamo, J. Jaramillo, R. Gomperts, R. E. Stratmann, O. Yazyev, A. J. Austin, R. Cammi, C. Pomelli, J. W. Ochterski, R. L. Martin, K. Morokuma, V. G. Zakrzewski, G. A. Voth, P. Salvador, J. J. Dannenberg, S. Dapprich, A. D. Daniels, O. Farkas, J. B. Foresman, J. V. Ortiz, J. Cioslowski, and D. J. Fox, *Gaussian 09, Revision D.01*, Gaussian, Inc., Wallingford CT, 2013.
19 (*a*) A. D. Becke, *J. Chem. Phys.*, 1993, **98**, 5648–5652; (*b*) C. Lee, W. Yang and R. G. Parr, *Phys. Rev. B: Condens. Matter Mater. Phys.*, 1988, **37**, 785–789; (*c*) P. J. Stephens, F. J. Devlin, C. F. Chabalowski and M. J. Frisch, *J. Phys. Chem.*, 1994, **98**, 11623–11627.
20 A. O. Terent'ev, M. M. Platonov, E. J. Sonneveld, R. Peschar, V. V. Chernyshev, Z. A. Starikova and G. I. Nikishin, *J. Org. Chem.*, 2007, **72**, 7237.
21 L. C. Crowley, G. Chojnowski and N. J. Waterhouse, *Cold Spring Harb. Protoc.*, 2016, DOI: 10.1101/pdb.prot087247.